Localization With Distributed MIMO Using a High-Speed Sigma-Delta-Over-Fiber Testbed

Citation for the original published paper (version of record):
Keskin, F., Sezgin, I., Bao, H. et al (2022). Localization With Distributed MIMO Using a High-Speed Sigma-Delta-Over-Fiber Testbed. IEEE Microwave and Wireless Components Letters, In Press.
http://dx.doi.org/10.1109/LMWC.2022.3157144

(article starts on next page)

Localization with Distributed MIMO Using a High-Speed Sigma-Delta-over-Fiber Testbed

Musa Furkan Keskin, *Member, IEEE*, Ibrahim Can Sezgin, Husileng Bao, *Member, IEEE*, Henk Wymeersch, *Senior Member, IEEE*, and Christian Fager, *Senior Member, IEEE*

***Abstract*—Distributed MIMO (D-MIMO) with synchronized access points (APs) is a promising architecture for both communications and localization in 5G and beyond systems. In this letter, we develop a time-difference-of-arrival (TDOA) based indoor localization system using a 2.35 GHz high-speed sigma-delta-over-fiber (SDoF) D-MIMO testbed with 40 MHz bandwidth, exploiting the fully synchronized nature of the APs. Experimental results over an area of size 100 m^2 demonstrate accuracies below 0.2 m and agree with the theoretical Cramér-Rao bounds at most measurement locations, indicating the localization capability of high-speed SDoF D-MIMO.**

***Index Terms*– Distributed MIMO, sigma-delta-over-fiber, synchronization, localization, Cramér-Rao bound.**

I. Introduction

Radio based localization relies on a variety of measurements including received signal strength (RSS), angle-of-arrival (AOA), time-of-arrival (TOA), and time-difference-of-arrival (TDOA) [1]. Commonly, localization is performed in two steps, where the first step estimates location-related measurements and the second step infers the unknown location based on those estimates [2]. In [3], a real-time FPGA implementation of an uplink TDOA measurement system using OFDM waveforms with Zadoff-Chu sequences is presented, with 1-D ranging accuracy of 8 cm using 40 MHz bandwidth. In [4], localization accuracies around 0.2 m are reported in a sub-6 GHz massive MIMO system by exploiting TOA, AOA and phase information under the assumption of perfect synchronization between the user equipment (UE) and the base station (BS). To improve channel richness and performance in future mobile networks [5], cell-free distributed MIMO (D-MIMO) arises as a promising alternative, which makes it interesting to explore also for precise localization purposes. In [6], an RSS-based downlink localization method is developed for a D-MIMO system, leading to errors above 5 m, while [7], [8] demonstrate TDOA-based uplink localization using D-MIMO with wirelessly synchronized access points (APs) and report accuracies on the order of 1 m using bandwidths from 20 MHz to 60 MHz. Moreover, the uplink TDOA-based D-MIMO system in [9] achieves accuracies down to 5.3 cm with 802.11g WiFi signals, but at the price of 10 GS/s sampling rate.

In this paper, we investigate the potential of D-MIMO for accurate TDOA based downlink localization of an unsynchronized UE in sub-6 GHz bands using a 2.35 GHz all-digital sigma-delta-over-fiber (SDoF) D-MIMO testbed with 12 channels [10]. Compared to [3] and [9], our testbed offers much greater range and flexibility in AP placement (up to a range of 300 m via optical fiber), while maintaining full downlink phase coherency. The all-digital architecture is also scalable to mmWave frequencies and larger bandwidths [11]. In addition, compared to [9], 140 MHz sampling rate of our system ensures low-cost implementation. We design transmit waveforms for APs, consisting of Golay and Zadoff-Chu sequences for coarse synchronization and fine delay estimation, respectively, and propose a TDOA based two-step localization algorithm by exploiting the full synchronization capability of the APs. To validate the effectiveness of the proposed approach, we perform anechoic chamber measurements and compare the experimental errors against the theoretical bounds. The results show that localization accuracies better than 0.2 m can be obtained with a 40 MHz signal (where the resolution is 7.5 m), demonstrating for the first time the potential of high-speed SDoF D-MIMO for indoor location-based applications.

Manuscript received December 22, 2021; revised February 17, 2022; accepted March 1, 2022. This work is supported by Chalmers Transport Area of Advance. M. F. Keskin and H. Wymeersch are with the Department of Electrical Engineering, Chalmers University of Technology, SE 41296 Gothenburg, Sweden (e-mail: {furkan, henkw}@chalmers.se). I. C. Sezgin is with Huawei Sweden, Stockholm, Sweden (e-mail: ibrahimcansezgin@gmail.com). H. Bao and C. Fager are with the Department of Microtechnology and Nanoscience, Chalmers University of Technology, SE-412 96 Gothenburg, Sweden (e-mail: {husileng,christian.fager}@chalmers.se).

II. Localization Algorithm

In this section, we describe the transmit signals employed for localization and propose a TDOA based two-step method to estimate the UE location.

A. Golay and Zadoff-Chu Sequences

We employ two different types of waveforms for the purpose of localization, as shown in Fig. 1. First, AP-1 transmits two Golay sequences of length 256 while the other APs remain idle to prevent interference at the UE. Golay sequences are used in the preamble of the IEEE 802.11ad waveform for frame synchronization [12] and thus enjoy favorable auto-correlation properties with low side-lobe levels. Therefore, they are ideally suited for ranging, i.e., coarse synchronization whereby the UE locks on to the AP transmission. Second, all APs simultaneously transmit orthogonal Zadoff-Chu (ZC) sequences [13] to enable estimation of pseudo-ranges[1] from different APs separately at the UE. The M-th root ZC sequence of length N is given by [13]

$$z_n = e^{-j\pi Mn(n+1)/N},\ n = 0, \ldots, N-1\ , \tag{1}$$

where N and M are relatively prime. The ZC sequences have the property that any non-zero circular shift leads to zero correlation with the original sequence [13], i.e.,

$$\sum_{n=0}^{N-1} z_n z^*_{[n+k]_{N-1}} = 0,\ k \neq 0\ , \tag{2}$$

where $[\cdot]_N$ denotes modulo-N. In the proposed D-MIMO implementation, we use $N = 7167$ and $M = 37$, and set the circular shift value between the ZC sequences of the different APs as $k = 240$. This corresponds to perfect correlation

[1]Due to clock bias between the APs and the UE, the estimated delays do not correspond to the true ranges, as opposed to [4].

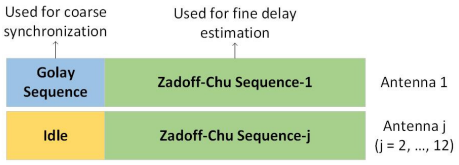

Fig. 1. Golay and Zadoff-Chu sequences.

between two AP transmissions only at the range difference of $1800\,\mathrm{m}$ at $40\,\mathrm{MHz}$ bandwidth (and zero correlation otherwise), which is far beyond the dimensions of interest in indoor localization.

B. TDOA Based Two-Step ML Estimator for Localization

Let $s_j(t)$ be the transmit signal from the j-th AP. Assuming line-of-sight (LOS) channel between each AP and the UE, the received signal at the UE can be expressed as [1]

$$r(t) = \sum_{j=1}^{N_{\mathrm{ap}}} \alpha_j s_j(t-\tau_j) + z(t) \ , \tag{3}$$

where N_{ap} is the number of APs, α_j and τ_j are the complex amplitude and the delay of the LOS path between the j-th AP and the UE, respectively, and $z(t)$ denotes noise and multipath interference. Considering equal-length fiber-optical interconnects and the full synchronization of the APs through accurately synchronized SDoF links, the path delays can be written as

$$\tau_j = \frac{\|\mathbf{p}-\mathbf{p}_j\| + b}{c} \ , \tag{4}$$

where c is the speed of propagation, $\mathbf{p}$ and $\mathbf{p}_j$ denote, respectively, the unknown UE location and the known location of the j-th AP, and b is the unknown time offset in terms of distance due to clock asynchronism between the master clock (CU clock) and the UE. In this part, we propose a two-step estimator [2] where the first step extracts $\{\tau_j\}_{j=1}^{N_{\mathrm{ap}}}$ (i.e., pseudo-ranges between the APs and the UE), and the second step estimates the UE location $\mathbf{p}$ using TDOA measurements.

1) Step 1 - Delay Estimation: At the receiver, we first synchronize to the AP transmission by identifying the arrival time of the Golay sequence transmitted by AP-1, which is simply performed via matched filtering, an example of which is shown in Fig. 2(a). Next, choosing the synchronization point as reference, we find the maximum-likelihood (ML) estimate of τ_j by matched filtering with the ZC sequence of the j-th AP signal for $j = 1, \ldots, N_{\mathrm{ap}}$. Fig. 2(b) plots an example result of correlation with the AP-1 ZC sequence, where the peaks of the other APs are also visible with an inter-peak distance of $1800\,\mathrm{m}$, as expected.

2) Step 2 - Position Estimation: Let $\widehat{\tau}_j$ denote the estimate of τ_j in (4), obtained at the output of Step 1. Following [14], the Cramér-Rao bound (CRB) on delay estimation can be expressed as

$$\mathbb{E}\{(\widehat{\tau}_j - \tau_j)^2\} \geq \lambda_j^{-1} \ , \tag{5}$$

where $\widehat{\tau}_j$ is an unbiased estimate of τ_j and $\lambda_j \triangleq \frac{8\pi^2\beta_j^2}{c^2}\mathrm{SNR}_j$, with β_j and SNR_j denoting the effective bandwidth of $s_j(t)$ [1] and the SNR from the j-th AP, respectively. Using the asymptotic unbiasedness and efficiency properties of the first-step ML estimates [15], the asymptotic distribution of $\widehat{\boldsymbol{\tau}} = \left[\widehat{\tau}_1 \ \ldots \ \widehat{\tau}_{N_{\mathrm{ap}}}\right]^T$ as SNR_j and/or β_j becomes sufficiently large is obtained as

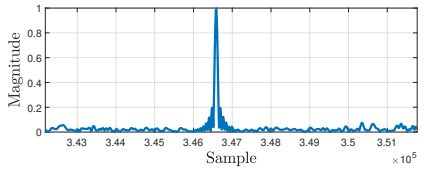

(a)

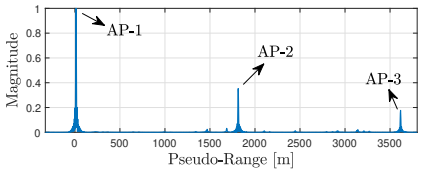

(b)

Fig. 2. (a) Coarse synchronization using Golay sequences and (b) range estimation using mutually orthogonal ZC sequences, where the received signal is correlated with the AP-1 sequence, leading to a pseudo-range estimate of $12.54\,\mathrm{m}$.

$$\widehat{\boldsymbol{\tau}} \sim \mathcal{N}(\boldsymbol{\tau}, \boldsymbol{\Sigma}) \ , \tag{6}$$

where $\boldsymbol{\tau} = \left[\tau_1 \ \ldots \ \tau_{N_{\mathrm{ap}}}\right]^T$ and $\boldsymbol{\Sigma} = \mathrm{diag}\left(\lambda_1^{-1}, \ldots, \lambda_{N_{\mathrm{ap}}}^{-1}\right)$.

In Step 2, to eliminate the clock offset b in (4), we choose the i-th AP (say, $i = 1$) as reference and create TDOA measurements from the delays $\{\widehat{\tau}_j\}_{j=1}^{N_{\mathrm{ap}}}$ as $\widehat{\Delta}\tau_j = \widehat{\tau}_j - \widehat{\tau}_i$, $j \in \mathcal{I}_i \triangleq \{1, \ldots, N_{\mathrm{ap}}\} \setminus \{i\}$. The asymptotic distribution of the TDOA measurement vector $\widehat{\boldsymbol{\Delta}}\tau = \left[\widehat{\Delta}\tau_1, \ldots, \widehat{\Delta}\tau_{N_{\mathrm{ap}}}\right]^T \in \mathbb{R}^{(N_{\mathrm{ap}}-1)\times 1}$ can be obtained as

$$\widehat{\boldsymbol{\Delta}}\tau \sim \mathcal{N}(\boldsymbol{\Delta\tau}, \boldsymbol{\Sigma}_{\boldsymbol{\Delta\tau}}) \ , \tag{7}$$

where $\boldsymbol{\Delta\tau} = \left[\Delta\tau_1, \ldots, \Delta\tau_{N_{\mathrm{ap}}}\right]^T \in \mathbb{R}^{(N_{\mathrm{ap}}-1)\times 1}$, $\boldsymbol{\Sigma}_{\boldsymbol{\Delta\tau}} = \mathrm{diag}\left(\{\lambda_j^{-1}\}_{j\in\mathcal{I}_i}\right) + \lambda_i^{-1}\mathbf{1}$. Here, $\Delta\tau_j = \tau_j - \tau_i$ and $\mathbf{1} \in \mathbb{R}^{(N_{\mathrm{ap}}-1)\times(N_{\mathrm{ap}}-1)}$ is the all-ones matrix. Based on (7), the ML position estimator can be straightforwardly derived as

$$\widehat{\mathbf{p}} = \arg\min_{\mathbf{p}} \ (\widehat{\boldsymbol{\Delta}}\tau - \boldsymbol{\Delta\tau})^T \boldsymbol{\Sigma}_{\boldsymbol{\Delta\tau}}^{-1} (\widehat{\boldsymbol{\Delta}}\tau - \boldsymbol{\Delta\tau}) \ , \tag{8}$$

where $\boldsymbol{\Delta\tau}$ is a function of the unknown UE location $\mathbf{p}$.

III. Localization Experiments with D-MIMO Testbed

In this section, we describe the experiments used to evaluate the performance of the proposed localization algorithm.

A. D-MIMO Testbed

As mentioned, the experiments rely on a flexible and low-cost SDoF D-MIMO testbed with simple off-the shelf optical link hardware [10] (shown in Fig. 3), supporting up to 12 fully phase coherent APs with non-directive antenna elements and an average output power of ca. 15 dBm each, which is slightly backed off to ensure linear operation. Standard equal-length optical fiber interconnects are used to connect the APs to a central processor (FPGA), where the arbitrary AP waveforms up to 40 MHz bandwidth can be generated and digitally upconverted to 2.35 GHz [10]. The modulated RF signal is recovered at each AP using a bulk-acoustic-wave (BAW) bandpass filter with an insertion loss less than 2 dB

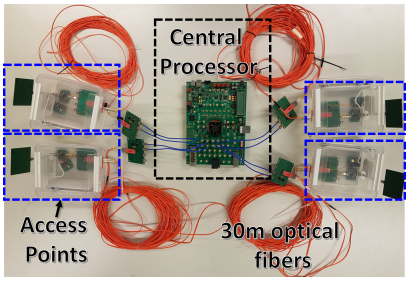

Fig. 3. Fully phase coherent D-MIMO testbed with multiple access points connected to a central station through 30m fiber-optical interconnects.

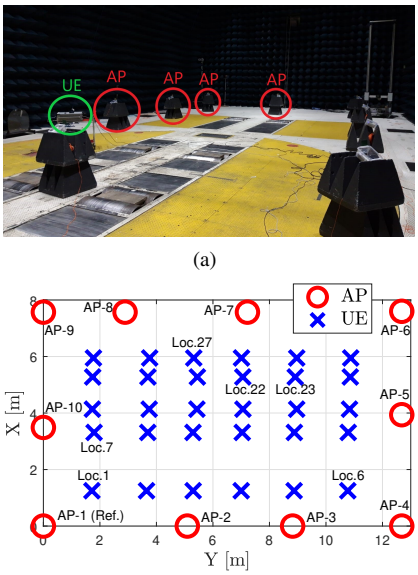

Fig. 4. (a) Anechoic chamber setup for localization experiments with D-MIMO testbed, and (b) configuration of APs and measurement locations for UE.

at the passband (2300–2400 MHz) and a minimum rejection of 20 dB at the stopband (10–2170 MHz and 2427–7200 MHz) [10]. The UE is, in these experiments, represented by a vector signal analyzer instrument (Keysight PXA 9030A). The transmit- and receive data is exchanged with the central processor and UE, respectively, using a LAN interface.

B. Experimental Setup

The localization experiments have been performed in an anechoic chamber inside the RiSE facility in Borås, Sweden. Fig. 4(a) shows the D-MIMO testbed with 10 APs and a UE in the anechoic chamber. Following the localization algorithm described in the previous section, the localization measurements have been taken at 30 different UE locations with a fixed configuration of APs, as shown in Fig. 4(b). The size of the area covered by the APs is approximately 100 m^2. The height of the APs is 1.06 m, while the height of the UE is 1.02 m. In this setup, location estimation has been performed on X-Y plane assuming the height of the UE is known a-priori.

C. Localization Results

In Fig. 5, we show the localization root mean-squared-errors (RMSEs) and the corresponding CRBs computed using [1, Thm. 1 & Thm. 4] at all measurement locations depicted in Fig. 4(b). It is seen that the errors vary between 0.15 m and 0.64 m, with the mean value of 0.42 m. The proposed TDOA

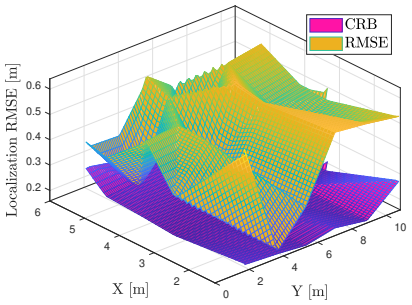

Fig. 5. Localization RMSEs and corresponding CRBs at all measurement locations in Fig. 4(b) using D-MIMO testbed.

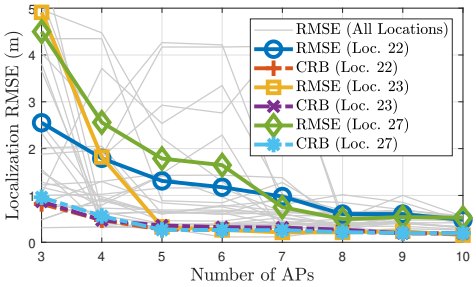

Fig. 6. Localization RMSEs and corresponding CRBs at different UE locations with respect to the number of APs.

based localization algorithm can attain the CRB at several locations, while performance gaps on the order of 0.1 m can arise, which might be due to uncalibrated hardware delays and/or ground reflections leading to unresolvable multipath components.

To evaluate the performance as a function of the number of APs used for location estimation, Fig. 6 illustrates the localization RMSEs and CRBs at various UE locations with respect to the number of APs[2]. We observe that the RMSE decreases with an increasing number of APs in general and can achieve the CRB when at least 5 APs are employed for localization. In addition, we investigate the effect of choosing a different ordering of APs, given by [1 3 7 10 5 9 4 6 8 2] (Order-2), on the localization performance. Since Order-2 provides a more homogeneous distribution of APs than Order-1 (see Fig. 4(b)), the resulting RMSEs for Order-2 are found to be lower than those for Order-1 for small number of APs. Due to unfavorable geometric arrangement of APs in Order-1, which is closely related to the concept of *geometric dilution of precision (GDOP)* [16] in GPS positioning, Order-1 leads to high RMSEs for small number of APs.

IV. Concluding Remarks

We have developed a new indoor localization system relying on a D-MIMO architecture that enables the usage of time-based measurements through synchronized APs. The proposed system provides synchronization by employing all-digital sigma-delta-over-fiber communication links. To localize the UE with multiple APs, we have designed mutually orthogonal transmit signals using ZC sequences and proposed a TDOA based two-step location estimator. The experimental results in an anechoic chamber have verified the effectiveness of the proposed localization system in indoor applications by showing accuracies below 0.2 m over an area of size 100 m^2.

[2]The indices of the APs (see Fig. 4(b)) that were chosen as the number of APs increases from 3 to 10 are [1 2 3 10 9 8 7 6 5 4] (Order-1).

REFERENCES

[1] Y. Shen and M. Z. Win, "Fundamental limits of wideband localization—part i: A general framework," *IEEE Transactions on Information Theory*, vol. 56, no. 10, pp. 4956–4980, 2010.

[2] S. Gezici, "A survey on wireless position estimation," *Wireless Personal Communications*, vol. 44, no. 3, pp. 263–282, 2008.

[3] G. Piccinni, G. Avitabile, G. Coviello, and C. Talarico, "Real-time distance evaluation system for wireless localization," *IEEE Transactions on Circuits and Systems I: Regular Papers*, vol. 67, no. 10, pp. 3320–3330, 2020.

[4] X. Li, E. Leitinger, M. Oskarsson, K. Åström, and F. Tufvesson, "Massive MIMO-based localization and mapping exploiting phase information of multipath components," *IEEE Transactions on Wireless Communications*, vol. 18, no. 9, pp. 4254–4267, 2019.

[5] J. Zhang, S. Chen, Y. Lin, J. Zheng, B. Ai, and L. Hanzo, "Cell-free massive MIMO: A new next-generation paradigm," *IEEE Access*, vol. 7, pp. 99 878–99 888, 2019.

[6] C. Liu, Z. Tian, M. Zhou, and X. Yang, "Gene-sequencing-based indoor localization in distributed antenna system," *IEEE Sensors Journal*, vol. 17, no. 18, pp. 6019–6028, 2017.

[7] J. Xiong, K. Jamieson, and K. Sundaresan, "Synchronicity: Pushing the envelope of fine-grained localization with distributed MIMO," in *Proceedings of the 1st ACM workshop on Hot topics in wireless*, 2014, pp. 43–48.

[8] J. Xiong, K. Sundaresan, and K. Jamieson, "Tonetrack: Leveraging frequency-agile radios for time-based indoor wireless localization," in *Proceedings of the 21st Annual International Conference on Mobile Computing and Networking*, 2015, pp. 537–549.

[9] C. Loyez, M. Bocquet, C. Lethien, and N. Rolland, "A distributed antenna system for indoor accurate WiFi localization," *IEEE Antennas and Wireless Propagation Letters*, vol. 14, pp. 1184–1187, 2015.

[10] I. C. Sezgin, M. Dahlgren, T. Eriksson, M. Coldrey, C. Larsson, J. Gustavsson, and C. Fager, "A low-complexity distributed-MIMO testbed based on high-speed sigma–delta-over-fiber," *IEEE Transactions on Microwave Theory and Techniques*, vol. 67, no. 7, pp. 2861–2872, 2019.

[11] C.-Y. Wu, H. Li, J. Van Kerrebrouck, A. Vandierendonck, I. L. de Paula, L. Breyne, O. Caytan, S. Lemey, H. Rogier, J. Bauwelinck, P. Demeester, and G. Torfs, "Distributed antenna system using sigma-delta intermediate-frequency-over-fiber for frequency bands above 24 GHz," *Journal of Lightwave Technology*, vol. 38, no. 10, pp. 2765–2773, 2020.

[12] P. Kumari, J. Choi, N. González-Prelcic, and R. W. Heath, "IEEE 802.11ad-based radar: An approach to joint vehicular communication-radar system," *IEEE Transactions on Vehicular Technology*, vol. 67, no. 4, pp. 3012–3027, April 2018.

[13] D. Chu, "Polyphase codes with good periodic correlation properties (corresp.)," *IEEE Transactions on Information Theory*, vol. 18, no. 4, pp. 531–532, 1972.

[14] S. Gezici and H. V. Poor, "Position estimation via ultra-wide-band signals," *Proceedings of the IEEE*, vol. 97, no. 2, pp. 386–403, 2009.

[15] H. V. Poor, *An Introduction to Signal Detection and Estimation*. Springer Science & Business Media, 2013.

[16] R. B. Langley *et al.*, "Dilution of precision," *GPS world*, vol. 10, no. 5, pp. 52–59, 1999.